Bioorganic & Medicinal Chemistry Letters 20 (2010) 5363–5375

Contents lists available at ScienceDirect

Bioorganic & Medicinal Chemistry Letters

journal homepage: www.elsevier.com/locate/bmcl

Bioorganic & Medicinal Chemistry Letters Volume 20, Issue 18, 2010

Contents

BMCL DIGEST

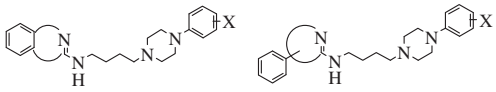

REGULAR ARTICLES

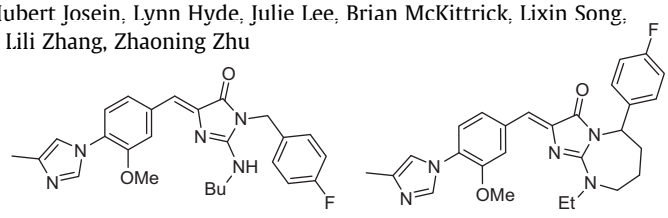

27 **39**

The synthesis of a novel series of iminoheterocycles and their structure–activity relationship (SAR) as modulators of γ-secretase activity will be detailed. Encouraging SAR generated from a monocyclic core led to a structurally unique bicyclic core. Selected compounds exhibit good potency as γ-secretase modulators, excellent rat pharmacokinetics, and lowering of $A\beta_{42}$ levels in various in vivo models.

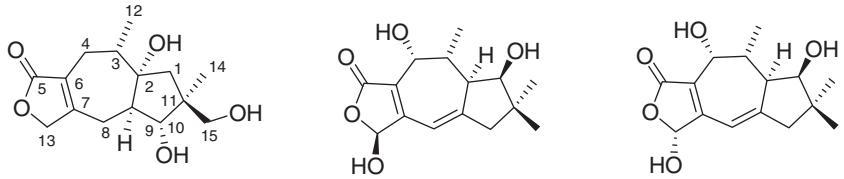

1 **2** **3**

Chemical investigation of the fruiting bodies of *Lactarius subvellereus* resulted in the isolation of three new lactarane sesquiterpenoids, subvellerolactones B (**1**), D (**2**), and E (**3**), together with four known lactarane sesquiterpenes (**4**–**7**).

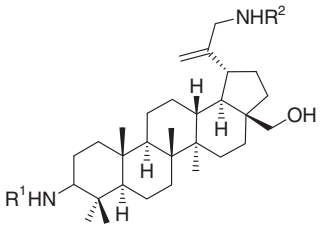

3,30-Bis(aza) derivatives were identified not only to possess improved cytotoxicity compared to the natural product betulinic acid but also to affect cell death predominantly via apoptosis, whereas the mono(aza) derivatives apparently triggered cell death via different, non-apoptotic pathway(s).

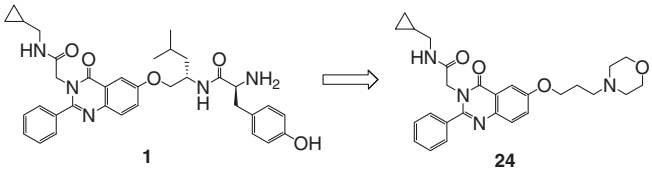

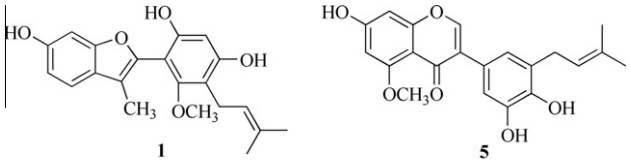

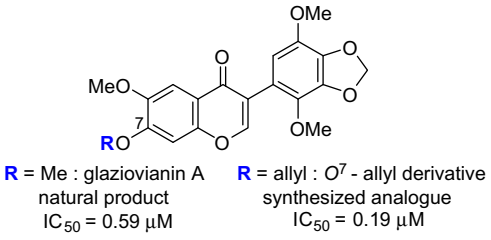

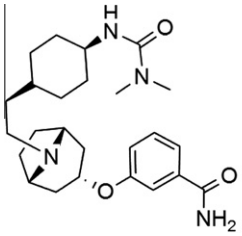

12

κ GTPγS IC_{50} = 172 nM
μ GTPγS IC_{50} = 16300 nM
δ GTPγS IC_{50} = >30000 nM

Additional SAR for an extended set of structural modification to key moieties of a novel series of selective kappa opioid receptor antagonists based on a previously disclosed series of 8-azabicyclo[3.2.1]octan-3-yloxybenzamides is described.

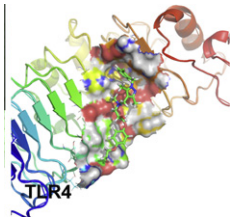

Increasing numbers of target protein structures available for computational studies makes the structure-based screening paradigm more attractive for initial hit indentification. We have developed a novel in silico screening methodology incorporating Molecular Mechanics (MM)/implicit solvent methods to evaluate binding free energies and applied this technology to the identification of inhibitors of the TLR4/MD-2 interaction.

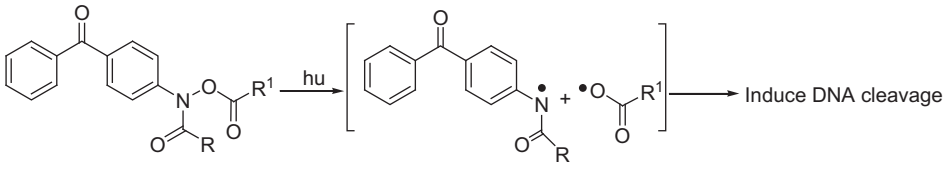

Efficient single strand DNA cleavage by acylaminyl radicals is reported.

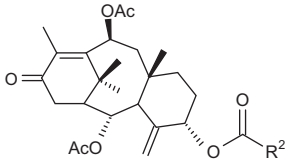

A series of new taxoids derived from sinenxan A were synthesized and evaluated for their in vitro multidrug resistant reversal activities. Four derivatives exhibited better activities than the positive control verapamil. Structure–activity relationships of these derivatives were explored as well.

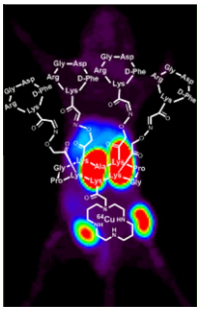

Positron emission tomography radiotracer was prepared by using a modular chemical strategy and applied to the non-invasive nuclear imaging of tumours.

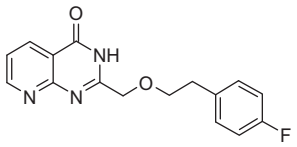

Pyrido pyrimidinones are selective agonists of the human high affinity niacin receptor GPR109A (HM74A). They show no activity on the highly homologous low affinity receptor GPR109B (HM74). Starting from a high throughput screening hit the in vitro activity of the pyrido pyrimidinones was significantly improved providing lead compounds suitable for further optimization.

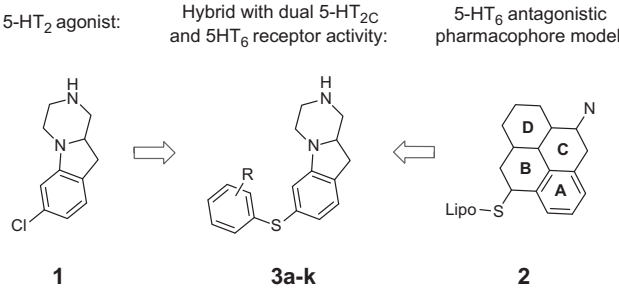

1 **3a-k** **2**

Novel 7-Phenylsulfanyl-1,2,3,4,10,10a-hexahydro-pyrazino[1,2-*a*]indoles **3a**–**k** are synthesized using a new and improved ring-closing methodology based on intramolecular C–H insertion of a carbene. The new compounds act as dual serotonin 5-HT$_{2C}$- and 5-HT$_6$-ligands.

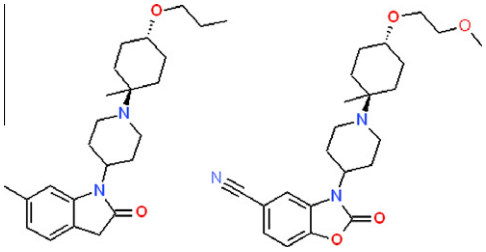

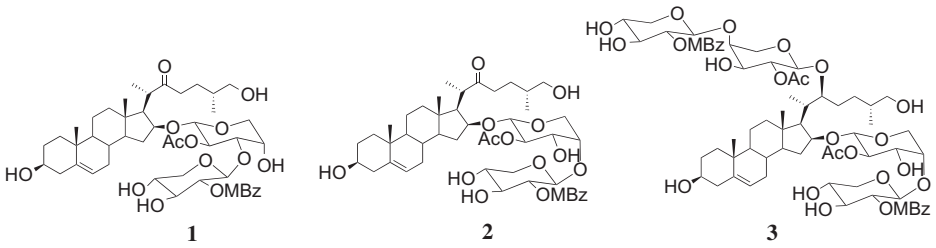

1 2 3

Three cholestane glycosides bearing the OSW-1 disaccharide or its 1→4-linked analogue were synthesized, and their cytotoxic activities were determined. Compound **1** showed potent cytotoxicity against five types of human tumor cells, with IC_{50} ranging between 1.3 and 73 nM.

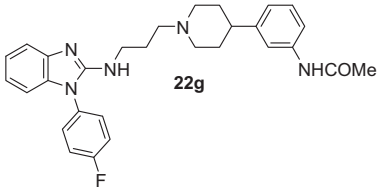

22g

The synthesis and biological evaluation of novel benzimidazole derivatives as MCHR1 antagonists are described. The in vivo proof of principle for weight loss is exemplified with compound **22g** from this series.

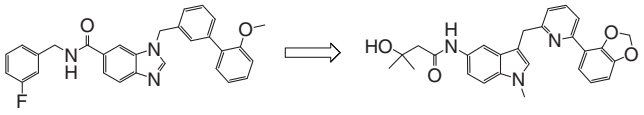

4
IC_{50} = 0.104 μM
AlogP = 5.63

18c
IC_{50} = 0.005 μM
AlogP = 3.60

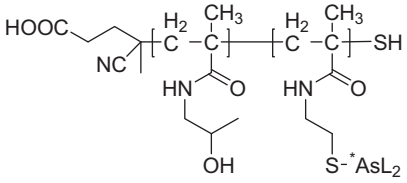

$^{72/74}$As labeling of thiol modified HPMA based polymers succeded in satisfying radiochemical yields of ~70%. These promsing results will enable long-term PET imaging in the close future.

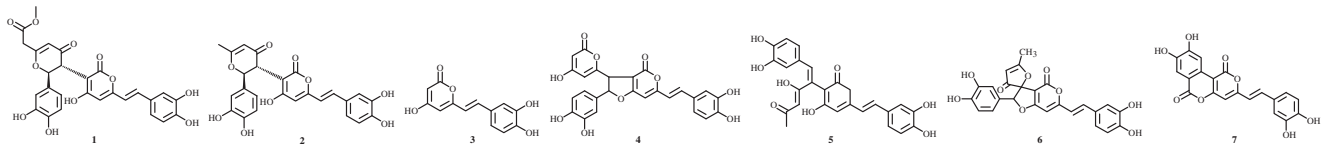

A new styrylpyrone, baumin, was isolated from the cultivated medicinal fungus *Phellinus baumii*, together with known compounds, davallialactone, hispidin, hypholomine B, interfungin A, inoscavin A, and phelligridin D, which were previously isolated from the medicinal fungi *Phellinus ignarius*, *Phellinus linteus*, and *Inonotus xeranticus*. Their structures were elucidated by extensive spectroscopic methods. These compounds exhibited antioxidant properties through Fenton reaction inhibition via iron chelation and free radical scavenging.

Among 23 3′,4′,5′-trimethoxychalcone analogues tested, some of the chalcones displayed potent antibacterial activity against *Helicobacter pylori*, in addition, **1**, **7**, and **13** showed the bactericide activity against the reference as well as multidrug-resistant strains. Additionally, **1**, **7**, and **13** potentially inhibited the *H. pylori*-induced inflammation in human gastric epithelial cells.

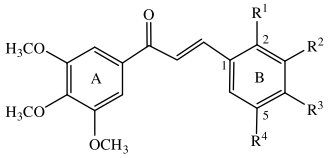

1. R^1 = OMe, R^2 = OMe, R^3 = H, R^4 = H

7. R^1 = H, R^2 = OMe, R^3 = OH, R^4 = H

13. R^1 = H, R^2 = H, R^3 = OMe, R^4 = H

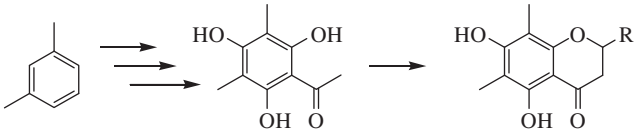

Synthetic route of target compounds

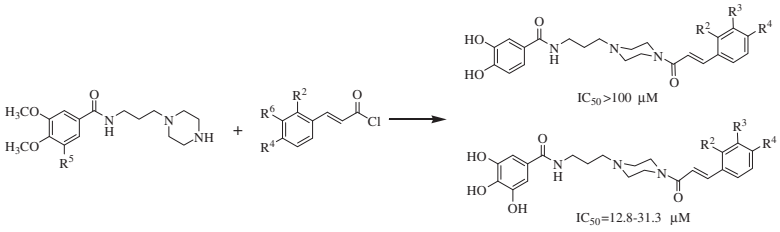

A series of polyhydroxylated aromatics having amidation of piperazine nitrogen were prepared and their HIV-1 IN inhibitory activities were evaluated. The galloyl moiety was a core pharmacophore in the inhibitory of HIV integrase.

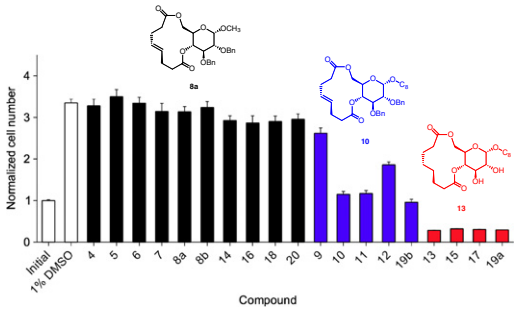

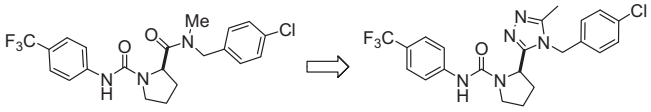

A novel series of pyrrolidine heterocycles was prepared and found to show potent inhibitory activity of CCR1 binding and CCL3 mediated chemotaxis of a CCR1-expressing cell line. A potent, optimized triazole lead from this series was found to have acceptable pharmacokinetics and microsomal stability in rat and is suitable for further optimization and development.

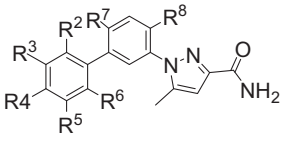

A series of low molecular weight biaryl substituted pyrazoles with good in-vitro potency and in-vivo efficacy were identified as $Na_v1.7$ blockers. These state dependent sodium channel blockers were synthesized and evaluated for treatment of neuropathic pain.

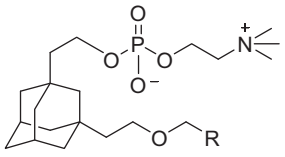

R = C_3H_7, C_5H_{11}, C_7H_{15}, C_9H_{19}, $C_{11}H_{23}$, C_6H_5

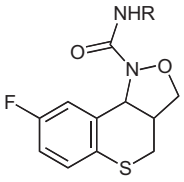

R = cyclohexyl

The serendipitous discovery of *N*-cyclohexyl-8-fluoro-3,3a,4,9b-tetrahydro-1*H*-thiochromeno[4,3-*c*]isoxazole-1-carboxamide as a selective human serotonin 5-HT$_{2B}$ antagonist with K_i of 42 ± 5 nM is reported herein. A subsequent functional assay indicated little agonist activity compared to 5-HT itself.

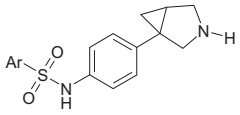

The new class of azabicyclo[3.1.0]benzensufonamides as selective dopamine D$_3$ antagonists is presented together with SAR and selectivity data.

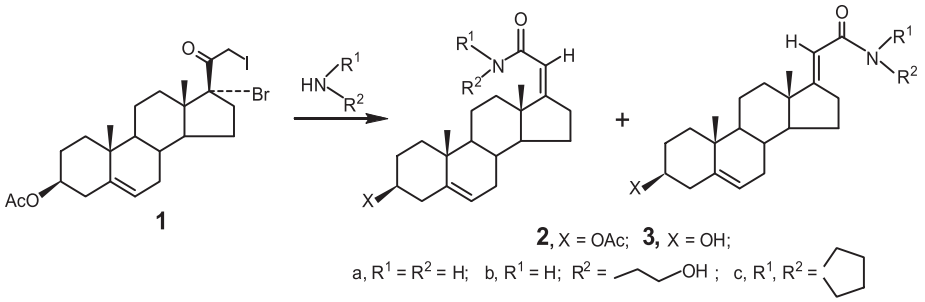

1

2, X = OAc; **3**, X = OH;

a, $R^1 = R^2 = H$; b, $R^1 = H$; R^2 = –(CH$_2$)$_3$–OH ; c, R^1, R^2 = –(CH$_2$)$_4$–

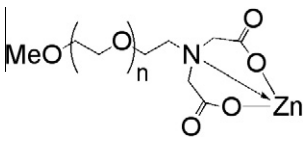

Successful nanoparticle-based delivery of siRNA requires shielding of particle surfaces from plasma proteins to allow sufficient circulation time. However, permanent PEGylation can inhibit cellular uptake. Herein, we report that nanoparticle stability can be enhanced through temporary zinc-mediated grafting of PEG to pre-formed nanoparticles.

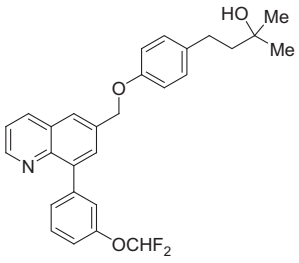

26b

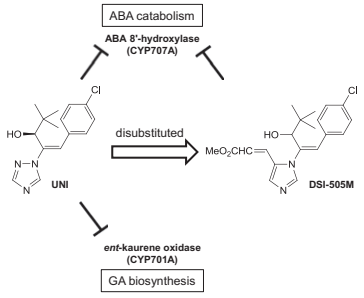

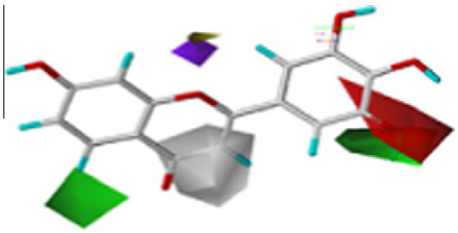

While the radical scavenging activity of galangin, 3,5,7-trihydroxyflavone was 52.5%, fisetin, 3,7,3′,4′-tetrahydroxyflavone showed 85.2%. To investigate the relationships between the structures of 30 hydroxyflavones and their antioxidative effects, the three-dimensional quantitative structure–activity relationships were examined.

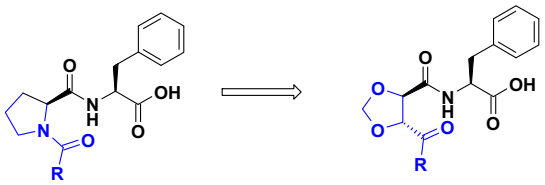

Pyrolidine ring in the *N*-acylphenylalanine class of VLA-4 antagonists has been successfully replaced by a 1,3-dioxolane and resulting derivative (**18e**) found to be potent in the series.

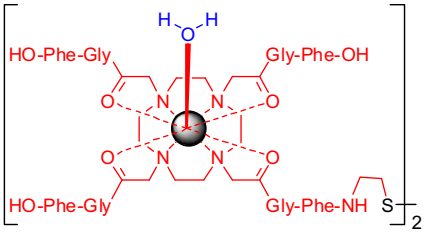

Synthesis and characterization of disulfide-bridged cell penetrating peptide conjugated and dimeric PARACEST MRI contrast agents based on DOTAM-Gly-L-Phe-OH scaffold.

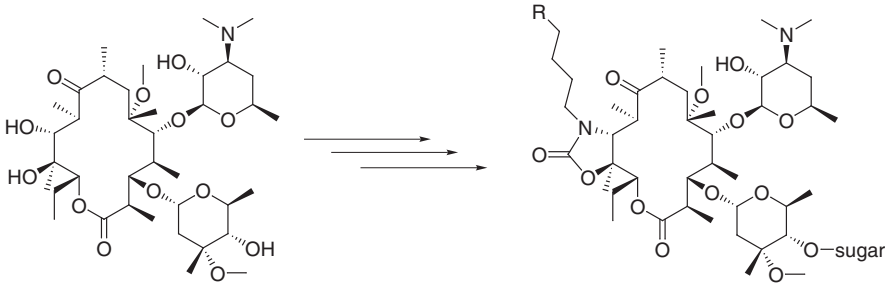

A novel series of macrolide derivatives with mono- or disaccharides substituted at the 4″-*O*- position has been synthesized, and their *in vitro* antibacterial activities were tested.

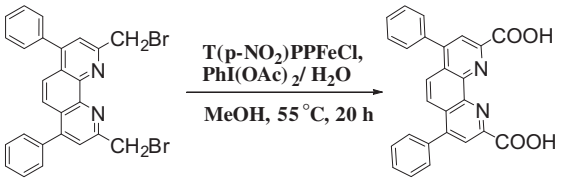

Using iron(III)porphyrins in combination with (diacetoxyiodo)benzene allows the conversion of 2,9-bis(bromomethyl)-4,7-diphenyl-1,10-phenanthroline into 4,7-diphenyl-1,10-phenanthroline -2,9-dicarboxylic acid in good yield. This method provides a cost-effective and environmentally-friendly oxidation procedure due to the utilization of less toxic $PhI(OAc)_2$ and biologically relevant iron(III)porphyrin.

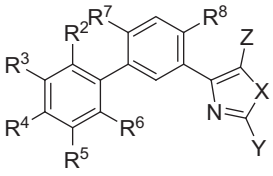

X = O, N or S

A series of low molecular weight biaryl substituted oxazoles, imidazoles, and thiazoles were identified as $Na_v1.7$ blockers. These state dependent sodium channel blockers were synthesized and evaluated for treatment of neuropathic pain.

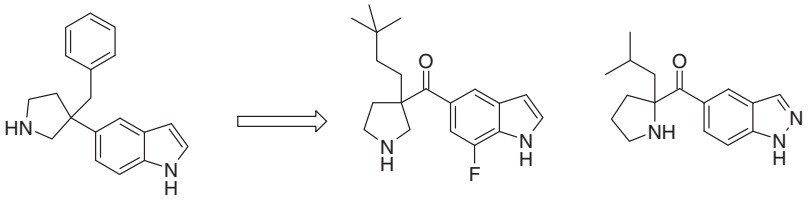

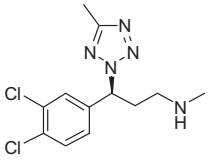

19r

A series of 3-aryl-3-azolylpropan-1-amines was prepared and screened for its capability of inhibiting monoamine reuptake. Analogs with nanomolar potency, good human in vitro microsomal stability, and low drug–drug interaction potential were described. In vivo models were used to evaluate the compound **19r** for antidepressive, anxiolytic, and analgesic activity.

A series of fluorine containing 4-(substituted-2-hydroxybenzoyl) pyrazoles and pyrazolyl benzo[*d*]oxazoles were synthesized and evaluated for their antibacterial activity against *Staphylococcus aureus*, *Escherichia coli*, *Pseudomonas aeruginosa* and *Bacillus subtilis* and antifungal activity against *Candida albicans*. The antibacterial activities were expressed as the minimum inhibitory concentration (MIC_{50}) in μg/ml. The compounds 1-(3,4-difluorophenyl)-4-(5-fluoro-2-hydroxybenzoyl)-1*H*-pyrazole (**4b**), oxime derivatives such as 1-(3,4-difluorophenyl)-1*H*-pyrazol-4-yl)(2-hydroxy-4-methylphenyl)methanone oxime (**5b**) and (5-chloro-2-hydroxyphenyl)(1-(3,4-difluorophenyl)-1*H*-pyrazol-4-yl)methanone oxime (**5e**) exhibited promising activities against tested bacterial strains. Except compound 1-(3,4-difluorophenyl)-4-(2-hydroxybenzoyl)-1*H*-pyrazole (**4d**), none of the other compounds showed promising antifungal activity.

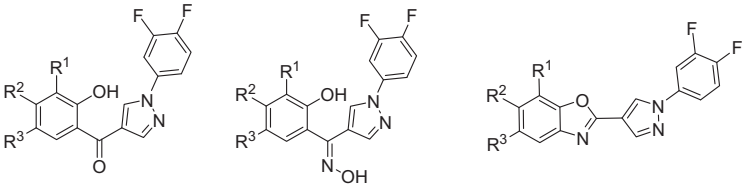

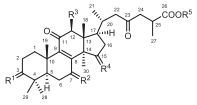

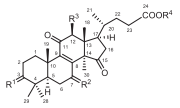

	R^1	R^2	R^3	R^4	R^5
1	O	βOH	H	αOH	Bu
2	βOH	βOH	H	O	Bu
5	O	βOH	H	αOH	H
6	O	βOH	H	αOH	Me
7	βOH	βOH	H	O	H
8	βOH	βOH	H	O	Me
9	O	βOH	H	O	Me
10	O	O	H	O	H
11	O	O	H	O	H
12	O	H_2	H	αOH	H
13	βOH	O	OAc	O	Me

	R^1	R^2	R^3	R^4
3	βOH	βOH	H	Bu
4	O	βOH	H	Bu
14	βOH	βOH	H	H
15	O	βOH	H	Me
16	βOH	βOH	OAc	Me
17	βOH	O	OAc	Me
18	O	O	H	Me

OTHER CONTENTS

*Corresponding author

ⓘ+ Supplementary data available via ScienceDirect

COVER

Overlay of high resolution co-crystal structures of *R*-**22**-ADP (cyan) and **1**-ADP (green) bound in an allosteric binding site of the mitotic kinesin KSP. [Roecker, A. J.; Coleman, P. J.; Mercer, S. P.; Schreier, J. D.; Buser, C. A.; Walsh, E. S.; Hamilton, K.; Lobell, R. B.; Tao, W.; Diehl, R. E.; South, V. J.; Davide, J. P.; Kohl, N. E.; Yan, Y.; Kuo, L. C.; Li, C.; Fernandez-Metzler, C.; Mahan, E. A.; Prueksaritanont, T.; Hartman, G. D. *Bioorg. Med. Chem. Lett.* **2007**, *17*, 5677.]

Indexed/Abstracted in: Beilstein, Biochemistry & Biophysics Citation Index, CANCERLIT, Chemical Abstracts, Chemistry Citation Index, Current Awareness in Biological Sciences/BIOBASE, Current Contents: Life Sciences, EMBASE/Excerpta Medica, MEDLINE, PASCAL, Research Alert, Science Citation Index, SciSearch, TOXFILE. Also covered in the abstract and citation database SCOPUS®. Full text available on ScienceDirect®

ELSEVIER

ISSN 0960-894X